Spatial gradients in the plasmasphere from Cluster

F. Darrouzet,[1] J. De Keyser,[1] P. M. E. Décréau,[2] J. F. Lemaire,[1] and M. W. Dunlop[3]

Received 10 January 2006; revised 15 February 2006; accepted 17 March 2006; published 26 April 2006.

[1] The Cluster mission allows the study of the plasmasphere with four-point measurements, including its overall density distribution, plasmaspheric plumes close to the plasmapause, and density irregularities inside the plasmasphere. The purpose of this letter is to examine the geometry and orientation of the overall density structure and of the magnetic field. We present a typical Cluster plasmasphere crossing for which we compute the four-point spatial gradient of the electron density and the magnetic field strength, and we compare the direction of both gradients with the local field vector. We discuss the role of the gradient components along and transverse to field lines; transverse density gradients, in particular, are found to suggest the presence of azimuthal density variations. **Citation:** Darrouzet, F., J. De Keyser, P. M. E. Decreau, J. F. Lemaire, and M. W. Dunlop (2006), Spatial gradients in the plasmasphere from Cluster, *Geophys. Res. Lett.*, *33*, L08105, doi:10.1029/2006GL025727.

1. Introduction

[2] The plasmasphere is a torus-shaped region surrounding the Earth, containing cold (a few eV or less) and dense ($10-10^4$ cm^{-3}) ions and electrons of ionospheric origin [*Lemaire and Gringauz*, 1998]. Density structures inside the plasmasphere have been observed by several spacecraft [*Chappell et al.*, 1970; *LeDocq et al.*, 1994; *Moldwin et al.*, 1995] and ground-based instruments [*Carpenter and Lemaire*, 1997]. More recently, small-scale plasmaspheric density structures have been observed onboard IMAGE by the Radio Plasma Imager [*Carpenter et al.*, 2002] and by the Extreme Ultraviolet imager [*Gallagher et al.*, 2005]. With the four-spacecraft Cluster mission, plasma density irregularities have been observed in the dusk sector by the WHISPER instrument [*Décréau et al.*, 2005] and also reported from direct observations of the ion distributions by the CIS experiment [*Dandouras et al.*, 2005]. A first statistical study of these structures has been made [*Darrouzet et al.*, 2004]. These structures are found over a broad range of spatial scales, with a transverse equatorial size from 20 to 5000 km.

[3] The Cluster mission allows the study of the geometry of these density structures and their orientation with respect to the magnetic field with high time resolution data at four nearby points. We analyze a typical plasmasphere crossing by Cluster with a four-point analysis tool: the spatial gradient of a scalar quantity. Except from computing derivatives of the magnetic field components to obtain curl(**B**) and div(**B**), in order to deduce electric current density [*Vallat et al.*, 2005; *Dunlop et al.*, 2006], no scalar gradient has been systematically computed yet, mainly because of calibration issues. This work analyzes a case study in depth, as a first step to improve this situation. After introducing the data set and the analysis technique in Section 2, the plasmasphere crossing is discussed in Section 3. Section 4 presents a summary and conclusions.

2. Data Sets and Analysis Technique

[4] The four Cluster spacecraft (C1, C2, C3, C4) cross the plasmasphere near perigee (around 4 R_E) every 57 hours from the Southern to the Northern Hemisphere. Two physical quantities are used in this study: electron density and magnetic field. The electron density is obtained from the WHISPER (Waves of HIgh frequency and Sounder for Probing Electron density by Relaxation) instrument [*Décréau et al.*, 2001]. In active mode, WHISPER unambiguously identifies the electron plasma frequency F_p [*Trotignon et al.*, 2003], which is related to the electron density N by:

$$F_p[\mathrm{kHz}] = 9\left(N\left[\mathrm{cm}^{-3}\right]\right)^{1/2}$$

F_p can also be inferred using WHISPER passive measurements by estimating the low frequency cut-off of natural plasma emissions [*Canu et al.*, 2001]. WHISPER operates between 2 and 80 kHz. We use the spin average DC magnetic field components measured by the FluxGate Magnetometer FGM [*Balogh et al.*, 2001]. To verify and interpret the results, we create a model magnetic field data set by evaluating a model that combines the internal magnetic field model IGRF2000 and the external magnetic field model Tsyganenko-96 [*Tsyganenko and Stern*, 1996] (computed with the UNILIB library, http://www.oma.be/NEEDLE/unilib.php/20x/) along the spacecraft trajectories.

[5] We compute the spatial gradient of a scalar quantity along the trajectory of the center of mass of the Cluster tetrahedron (method described by *Harvey* [1998]) from simultaneous measurements f^α ($\alpha = 1, \ldots, 4$) of a scalar quantity at the four satellites, postulating that their positions $\boldsymbol{x}^\alpha$ ($\alpha = 1, \ldots, 4$) are close enough to each other, so that all spacecraft are embedded in the same structure at the same time (homogeneity condition). The spatial gradient components $\partial f/\partial i$ for $i = x, y, z$ are then given by:

$$\frac{\partial f}{\partial i} = \frac{1}{2}\frac{1}{4^2}\sum_{j=x,y,z}\left[\sum_{\alpha=1}^{4}\sum_{\beta=1}^{4}\left(f^\alpha - f^\beta\right)\left(x_j^\alpha - x_j^\beta\right)\right] \times R_{ji}^{-1}$$

with R_{ji} the volumetric tensor $\frac{1}{4}\sum_{\alpha=1}^{4} x_j^\alpha x_i^\alpha$.

[1] Belgian Institute for Space Aeronomy (IASB-BIRA), Brussels, Belgium.
[2] Laboratoire de Physique et Chimie de l'Environnement (LPCE/CNRS), Orléans, France.
[3] Rutherford Appleton Laboratory (RAL), Oxon, UK.

0094-8276/06/2006GL025727$05.00

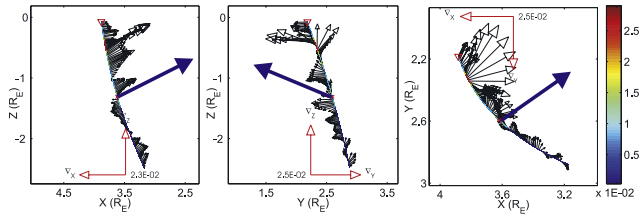

Figure 1. Density gradient vectors projected onto the XZ, YZ and XY GSE planes during the inbound plasmasphere crossing between 07:00 and 08:00 UT on 7 August 2003. The color scale corresponds to the magnitude of the gradient along the trajectory. The blue arrows point toward the Earth.

[6] The computation of a spatial gradient is inherently a difficult operation: It involves calculating the differences of quantities that are similar, and thus results in large relative errors. These errors may be anisotropic, depending on the nature of the spacecraft configuration, as reflected by the volumetric tensor and by the covariance matrix of the error in the determination of the spacecraft position [*Chanteur and Harvey*, 1998]. In addition, the homogeneity condition requires the spacecraft to be close together relative to the size of the physical structure one intends to examine. In that case, the differences between simultaneously measured f^{α} are very small, resulting in a large error on the gradient. To reduce such errors, we filter away any variations at time scales commensurate with length scales shorter than what we are interested in, by smoothing the scalar profiles prior to computing the gradient. As the gradient can be computed for any scalar quantity, it is natural to do so for the electron density obtained from WHISPER's plasma frequency, with its inherent absolute calibration and high measurement frequency resolution of 163 Hz, and for the magnetic field strength from FGM, which is measured with an uncertainty of less than 0.1 nT and which has an inter-calibration error below that value.

3. A Typical Plasmasphere Crossing

[7] We study the plasmasphere crossing on 7 August 2003, between 07:00 and 09:00 UT, at 14:00 LT and between $-30°$ and $30°$ of magnetic latitude. The maximum value of K_p in the previous 24 hours was 2^+, implying a geomagnetically moderately active regime. The spacecraft separation is small (200 × 400 × 1000 km in X, Y, Z GSE directions) and the tetrahedron geometric factors are satisfactory: elongation of 0.85 and planarity between 0.5 and 0.8 (see *Robert et al.* [1998] for detailed explanations about those quantities). The density gradient ∇N on the inbound part of the crossing (Figure 1) is generally toward Earth, with some azimuthal deviations (visible in the XY plane). During the outbound part of the crossing (not shown), the gradient is less regular. The corresponding density profiles are shown in Figure 2a. The magnetic field strength gradient ∇B is very regular, always toward the Earth. By estimating the approximation error on the gradient (related to the homogeneity condition), as well as the error due to measurements uncertainties, we can determine the total error on the gradients: It is 15% for ∇N and 5% for ∇B.

[8] The angles of ∇N and ∇B with respect to the local magnetic field **B** (at the center of mass of the tetrahedron), α_{BN} and α_{BB}, are plotted in Figure 2b (red and blue curves, respectively). Both angles range between 0° and 90°, because we are only interested in the orientation of the gradients, and not in their sense. Making abstraction of the anisotropy of the errors, the orientation of both gradients is known up to a precision of 9° for ∇N and 3° for ∇B. This is in particular the case for the angles α_{BN} and α_{BB}. The global orientation of the density gradient is also described by its latitude angle $\theta_{\nabla N}$ and its azimuth angle relative to the spacecraft azimuth angle $\phi_{\nabla N} - \phi_{sc}$ in GEO, plotted in Figures 2c–2d (red). The latitude angle $\theta_{\nabla B}$ and azimuth angle $\phi_{\nabla B} - \phi_{sc}$ of the gradient of the observed FGM magnetic field (blue, solid curves), as well as of the IGRF2000-Tsyganenko model field (blue, dashed curves) are displayed on the same panels. The precision is 9° on $\theta_{\nabla N}$ and $\phi_{\nabla N} - \phi_{sc}$ and 3° on $\theta_{\nabla B}$ and $\phi_{\nabla B} - \phi_{sc}$.

[9] The magnetic equator, defined as the surface of minimum field strength locations along field lines, is crossed where $\boldsymbol{B}$ and $\nabla \boldsymbol{B}$ are perpendicular, i.e., $\alpha_{BB} = 90°$. This allows an unambiguous identification of the time of crossing of the magnetic equator in Figure 2b at 08:03 UT. Note that this in general does not coincide with

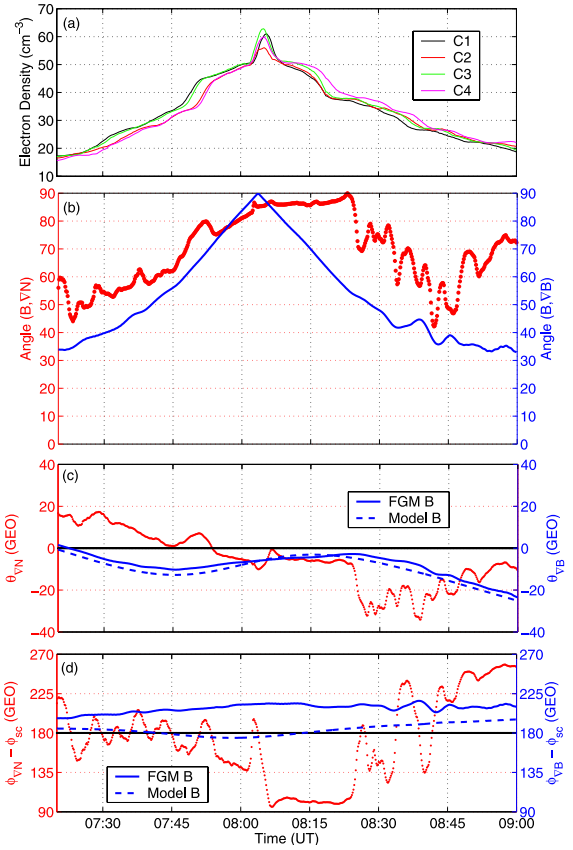

Figure 2. (a) Electron density from WHISPER onboard the four Cluster spacecraft, (b) α_{BB} (blue curve) and α_{BN} (red dots), (c) latitude angle θ_{∇} and (d) azimuth angle $\phi_{\nabla} - \phi_{sc}$ of the density gradient (red) and magnetic field strength gradient (blue), as a function of time during the plasmasphere crossing on 7 August 2003. The angles related to the density gradient ∇N are known up to 9°, and the angles related to the magnetic field gradient ∇B up to 3°.

the time of perigee or with the time of maximum density, but there is not much difference in the present case.

[10] Before and after crossing the magnetic equator, the spacecraft sample field lines farther away from the equator and α_{BB} decreases as B increases along a field line in the poleward direction in a progressively steeper fashion. Far from the magnetic equator, α_{BB} becomes more variable; the spacecraft are then in the outer fringes of the plasmasphere, where the magnetic field strength is smaller and plasma β is higher, which could enhance diamagnetic effects.

[11] For both the observed magnetic field (FGM data) and the model field (IGRF-Tsyganenko), the values of $\theta_{\nabla B}$ are comparable; they vary between 0° and −20°. For a tilted dipole (tilt of 10.3° at 71.7°W longitude in 2003), at 08:03 UT and 14:00 LT, the magnetic equator should be at a latitude of 10°; for the actually observed magnetic field, the spacecraft encounter the magnetic equator at $\theta_{sc} = 8.5°$ (spacecraft position at 08:03 UT), which is in fair agreement. At the magnetic equator of an exact dipole, $\boldsymbol{\nabla B}$ would point earthward, so that $\theta_{\nabla B} = -\theta_{sc}$; at the actual magnetic equator, the observed value is $\theta^{eq}_{\nabla B} = -6°$, consistent with a dipole somewhat skewed in the North–South direction.

[12] When the Cluster spacecraft cross field lines at higher latitude, the variation of $\theta_{\nabla B}$ depends on how fast B increases away from the magnetic equator. Noting that the spacecraft remain at approximately the same LT, Figure 2b indicates that α_{BB} decreases rapidly, so that $\theta_{\nabla B} > \theta^{eq}_{\nabla B}$ just above the magnetic equator and $\theta_{\nabla B} < \theta^{eq}_{\nabla B}$ just below it. But since the field lines are curved toward the Earth farther away from the equator, ultimately $\theta_{\nabla B} \ll \theta^{eq}_{\nabla B}$ at higher latitudes above the magnetic equator and $\theta_{\nabla B} \gg \theta^{eq}_{\nabla B}$ below it. The actual behavior of $\theta_{\nabla B}$ is determined by the geometry of the field lines and by the interplay between the variation of B along field lines ($\nabla_{\parallel} B$) and its variation across field lines ($\nabla_{\perp} B$), offset by the overall dipole tilt.

[13] The gradient of the observed magnetic field (FGM data) has $\phi_{\nabla B} - \phi_{sc} \approx 200°$, while it is around 180° for the gradient of the model field (IGRF-Tsyganenko). If the magnetic field would be a tilted dipole, one would expect $\phi_{\nabla B} - \phi_{sc} = 180°$ at the magnetic equator. The IGRF-Tsyganenko model represents a modified tilted dipole, and indeed has $\phi_{\nabla B} - \phi_{sc}$ close to 180°. The observed azimuth angle of 200° can only be explained by a deviation from cylinder symmetry around the dipole axis.

[14] Before 07:50 UT, between 07:55 and 08:00 UT, and after 08:25 UT, the density changes rather slowly; that is, the spacecraft see similar densities at a given time (Figure 2a), so that α_{BN} depends on the balance between the variations of density along field lines ($\nabla_{\parallel} N$) and across field lines ($\nabla_{\perp} N$) (see Figure 2b), similar to the behavior of α_{BB}. α_{BN} increases progressively as the spacecraft approach the magnetic equator, because of the absence of abrupt $\nabla_{\perp} N$. However, the curve is broader as $\nabla_{\parallel} N / \nabla_{\perp} N \ll \nabla_{\parallel} B / \nabla_{\perp} B$. For the same reason, $\theta_{\nabla N}$ varies from positive values in the Southern Hemisphere to negative values in the Northern Hemisphere, with a large central region where $\theta_{\nabla N} \approx 0°$ (Figure 2c). In the same regions of slow density variations, $\phi_{\nabla N} - \phi_{sc}$ is fluctuating around 180° (Figure 2d). This seems to indicate the existence of azimuthal ripples, which are similar to the structures described by *Bullough and Sagredo* [1970].

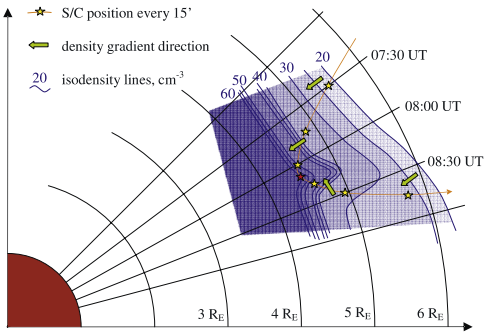

Figure 3. Sketch of the plasmasphere crossing projected onto the equatorial plane in a co-rotating frame centered on 08:00 UT and 14:00 LT, on 7 August 2003. The density gradient is inward during the inbound part of the crossing; it points azimuthally duskward for much of the outbound part.

[15] When the spacecraft observe markedly different densities at a given time (in the density step at 07:50–07:55 UT, and during the whole period 08:00–08:25 UT), the density gradients are definitely stronger (Figure 2a). This is due to an important contribution of $\nabla_{\perp} N$. Then $\nabla_{\parallel} N \ll \nabla_{\perp} N$ there, so $\alpha_{BN} \approx 90°$ (Figure 2b) and $\theta_{\nabla N} \approx 0°$ (Figure 2c). These gradients correspond to transverse density structure, as noticed before in the density gradient projections (Figure 1).

[16] During the density step at 07:50–07:55 UT, $\phi_{\nabla N} - \phi_{sc}$ is close to 180° (Figure 2d), showing that the spacecraft cross perpendicularly through this density interface, evident also in Figure 2a by the sequential passing of the spacecraft through the density step. However, during much of the outbound pass (08:00–08:25 UT), $\phi_{\nabla N} - \phi_{sc} \approx 90°$, indicating a crossing tangent to the density structure, visible in Figure 2a by the spacecraft remaining at different positions across the density interface for an extended time. The corresponding geometry in the equatorial plane is sketched in Figure 3. One can verify that, for these structures, the homogeneity condition is satisfied.

4. Summary and Conclusions

[17] We have presented the first systematic spatial gradient results from the four-spacecraft Cluster mission in the plasmasphere, thus providing the spatial gradient of density and magnetic field strength from well-calibrated, unbiased measurements. This produces a more complete view of the geometry of the outer plasmasphere. It allows the evaluation of the relative importance between the two effects influencing the spatial gradients inside the plasmasphere: the increase of the density and the magnetic field strength along the field lines away from the equator, and the decrease of these two quantities away from Earth.

[18] The variations of the magnetic field strength along the field lines are rather fast, with $\nabla_{\parallel} B > \nabla_{\perp} B$ (except very close to the magnetic equator). We find the latitudinal magnetic field structure to be compatible with a tilted dipole, but there appear to be significant deviations from cylindrical symmetry.

[19] The overall density structure is mainly aligned with the magnetic field at these magnetic latitudes (±30°) with pronounced transverse density structure. The density variations across the field lines are more pronounced than those

along the field lines, producing gradients with $\nabla_{\perp} N > \nabla_{\parallel} N$. From an IMAGE study, *Reinisch et al.* [2001] also found that the density does not change very much along a flux tube at low magnetic latitudes. The presence of the transverse density gradients makes it difficult to evaluate the effect of the magnetic field tilt on the density distribution. In any case, there is no evidence for sharp density gradients along field lines (the value of α_{BN} rarely drops below 50°), such as would be expected in shocks propagating along the field lines; this suggests that refilling of flux tubes is a gradual process as described by *Lemaire* [1989].

[20] There are limitations to the practical applicability of the gradient analysis techniques presented here. The upper limit (80 kHz) of the WHISPER instrument allows density measurements up to $N \approx 80$ cm^{-3}. On occasions when the Cluster spacecraft dive deeper into the plasmasphere (though always limited by the relatively high perigee at 4 R_E), higher densities can be derived from the spacecraft potential, with WHISPER aiding in calibrating the low density measurements. It remains, however, difficult to properly calibrate data at higher densities, rendering reliable gradient computations difficult in those cases. It should also be noted that the gradient computations are justified only when the homogeneity condition is satisfied.

[21] **Acknowledgment.** F. Darrouzet, J. De Keyser and J. F. Lemaire acknowledge the support by the Belgian Federal Services for Scientific, Technical, and Cultural Affairs and by the ESA/PRODEX Cluster project.

References

Balogh, A., et al. (2001), The Cluster Magnetic Field Investigation: Overview of in-flight performance and initial results, *Ann. Geophys.*, *19*, 1207–1217.

Bullough, K., and J. L. Sagredo (1970), Longitudinal structure in the plasmapause: VLF goniometer observations of knee-whistlers, *Nature*, *225*, 1038–1039.

Canu, P., et al. (2001), Identification of natural plasma emissions observed close to the plasmapause by the Cluster-Whisper relaxation sounder, *Ann. Geophys.*, *19*, 1697–1709.

Carpenter, D. L., and J. Lemaire (1997), Erosion and recovery of the plasmasphere in the plasmapause region, *Space Sci. Rev.*, *80*, 153–179.

Carpenter, D. L., et al. (2002), Small-scale field-aligned plasmaspheric density structures inferred from the Radio Plasma Imager on IMAGE, *J. Geophys. Res.*, *107*(A9), 1258, doi:10.1029/2001JA009199.

Chanteur, G., and C. C. Harvey (1998), Spatial interpolation for four spacecraft: Application to magnetic gradients, in *Analysis Methods for Multi-Spacecraft Data*, edited by G. Paschmann and P. W. Daly, *ISSI Sci. Rep. SR-001*, pp. 371–393, Int. Space Sci. Inst., Bern.

Chappell, C. R., K. K. Harris, and G. Sharp (1970), A study of the influence of magnetic activity on the location of the plasmapause as measured by OGO 5, *J. Geophys. Res.*, *75*, 50–56.

Dandouras, I., et al. (2005), Multipoint observations of ionic structures in the plasmasphere by CLUSTER-CIS and comparisons with IMAGE-EUV observations and with model simulations, in *Inner Magnetosphere Interactions: New Perspectives from Imaging*, *Geophys. Monogr. Ser.*, vol. 159, edited by J. L. Burch, M. Schulz, and H. Spence, pp. 23–53, AGU, Washington, D. C.

Darrouzet, F., et al. (2004), Density structures inside the plasmasphere: Cluster observations, *Ann. Geophys.*, *22*, 2577–2585.

Décréau, P. M. E., et al. (2001), Early results from the Whisper instrument on Cluster: An overview, *Ann. Geophys.*, *19*, 1241–1258.

Décréau, P. M. E., et al. (2005), Density irregularities in the plasmasphere boundary player: Cluster observations in the dusk sector, *Adv. Space Res.*, *36*, 1964–1969.

Dunlop, M. W., et al. (2006), The Curlometer and other gradient measurements with Cluster, in *Proceedings of the Cluster and Double Star Symposium: 5th Anniversary of Cluster in Space*, *Eur. Space Agency Spec. Publ.*, *ESA SP-598*.

Gallagher, D. L., M. L. Adrian, and M. W. Liemohn (2005), Origin and evolution of deep plasmaspheric notches, *J. Geophys. Res.*, *110*, A09201, doi:10.1029/2004JA010906.

Harvey, C. C. (1998), Spatial gradients and the volumetric tensor, in *Analysis Methods for Multi-Spacecraft Data*, edited by G. Paschmann and P. W. Daly, *ISSI Sci. Rep. SR-001*, pp. 307–322, Int. Space Sci. Inst., Bern.

LeDocq, M. J., D. A. Gurnett, and R. R. Anderson (1994), Electron number density fluctuations near the plasmapause observed by the CRRES spacecraft, *J. Geophys. Res.*, *99*, 23,661–23,671.

Lemaire (1989), Plasma distribution models in a rotating magnetic dipole and refilling plasmaspheric flux tubes, *Phys. Fluids*, *32*, 1519–1527.

Lemaire, J. F., and K. I. Gringauz (Eds.) (1998), *The Earth's Plasmasphere*, 372 pp., Cambridge Univ. Press, New York.

Moldwin, M. B., M. F. Thomsen, S. J. Bame, D. McComas, and G. D. Reeves (1995), The fine-scale structure of the outer plasmasphere, *J. Geophys. Res.*, *100*, 8021–8030.

Reinisch, B. W., X. Huang, P. Song, G. S. Sales, S. F. Fung, J. L. Green, D. L. Gallagher, and V. M. Vasyliunas (2001), Plasma density distribution along the magnetospheric field: RPI observations from IMAGE, *Geophys. Res. Lett.*, *28*, 4521–4524.

Robert, P., A. Roux, C. C. Harvey, M. W. Dunlop, P. W. Daly, and K.-H. Glassmeier (1998), Tetrahedron geometric factors, in *Analysis Methods for Multi-Spacecraft Data*, edited by G. Paschmann and P. W. Daly, *ISSI Sci. Rep. SR-001*, pp. 323–348, Int. Space Sci. Inst., Bern.

Trotignon, J. G., P. M. E. Décréau, J. L. Rauch, E. Le Guirriec, P. Canu, and F. Darrouzet (2003), The Whisper relaxation sounder onboard Cluster: A powerful tool for space plasma diagnosis around the Earth, *Cosmic Res.*, *41*, 369–372.

Tsyganenko, N. A., and D. P. Stern (1996), Modeling the global magnetic field of the large-scale Birkeland current systems, *J. Geophys. Res.*, *101*, 27,187–27,198.

Vallat, C., et al. (2005), First current density measurements in the ring current region using simultaneous multi-spacecraft Cluster-FGM data, *Ann. Geophys.*, *23*, 1849–1865.

F. Darrouzet, J. De Keyser, and J. F. Lemaire, Belgian Institute for Space Aeronomy (IASB-BIRA), 3 Avenue Circulaire, B-1180 Brussels, Belgium. (fabien.darrouzet@oma.be; johan.dekeyser@oma.be; joseph.lemaire@oma.be)

P. M. E. Décréau, Laboratoire de Physique et Chimie de l'Environnement (LPCE/CNRS), 3A, Avenue de la Recherche Scientifique, F-45071 Orléans Cedex 2, France. (pdecreau@cnrs-orleans.fr)

M. W. Dunlop, Rutherford Appleton Laboratory (RAL), Oxon OX11 0QX, UK. (m.w.dunlop@rl.ac.uk)